JOURNAL OF COMPUTATIONAL PHYSICS 119, 188–194 (1995)

Mesh Effects for Rossby Waves*

JOHN K. DUKOWICZ

Theoretical Division, Group T-3, Los Alamos National Laboratory, University of California, Los Alamos, New Mexico 87545

Received August 3, 1994; revised December 27, 1994

Dispersion relations are obtained for Rossby waves on Arakawa grids A–E. The discretization accuracy is compared for both inertia–gravity and Rossby waves in terms of "domains of accuracy" for a given level of percentage error. In particular, the B-grid appears to be superior to the C-grid for the case of both resolved and underresolved Rossby radius. This is in contrast to the well-known situation for inertia–gravity waves where the B-grid is inferior for the case of resolved Rossby radius. © 1995 Academic Press, Inc.

1. INTRODUCTION

Winninghoff [1] and Arakawa and Lamb [2] analyzed the dispersion error for the numerical discretization of inertia–gravity waves on five different grids, which have become known as the Arakawa A–E grids (Fig. 1) in the meteorological and oceanographic literature. The behavior of waves on different types of finite-difference grids gives great insight into the choice of a particular numerical grid and provides useful information about the suitability and accuracy of a grid for various types of problems. This subject has been of continuing interest as evidenced by the works of Batteen and Han [3], Song and Tang [4], and Randall [5], for example, who all considered inertia–gravity waves. However, it is not always clear that the choice of inertia–gravity waves is best for this type of analysis. Inertia–gravity waves are essential only in the process of geostrophic adjustment. Perhaps of equal if not greater interest are the Rossby (or planetary) wave dynamics which occur following the process of geostrophic adjustment. One is interested in Rossby wave dynamics to the extent that atmospheric or oceanic flows can be well represented by a quasi-geostrophic model, which is often the case. However, Rossby waves in the atmosphere are typically well resolved by the mesh. This is not so in the oceanic case where even the highest resolution computations currently do not resolve the first baroclinic Rossby radius. Thus, it is important and useful to analyze mesh effects for both inertia–gravity as well as Rossby waves.

The dispersion analysis for Rossby waves is not quite as straightforward as it is for inertia–gravity waves. Finite-difference Rossby wave dispersion relations for the B and C grids have been analyzed by Wajsowicz [6]. In this note we complete the analysis by giving analytic expressions and graphical representations for the discrete dispersion relations for all five grids and for both inertia–gravity and Rossby waves, and we present a novel comparison of the errors in terms of the "domains of accuracy." The analytical dispersion relations may then be used for further analysis, if so desired.

2. INERTIA–GRAVITY (POINCARÉ) WAVES

Here we review the now classic results in Arakawa and Lamb [2] and elsewhere. The linearized shallow water equations which describe inertia–gravity waves on an f-plane are given by

$$\begin{aligned} \partial_t u - fv + g\partial_x h &= 0, \\ \partial_t v + fu + g\partial_y h &= 0, \\ \partial_t h + H(\partial_x u + \partial_y v) &= 0, \end{aligned} \tag{1}$$

where (u, v) are the horizontal velocity components, and h is the displacement from a constant depth H. Assuming plane waves of the form $h \sim e^{i(kx+ly-\omega t)}$, we obtain the continuum (exact) dispersion relationship

$$\left(\frac{\omega}{f}\right)^2 = 1 + \left(\frac{\lambda}{d}\right)^2 [(kd)^2 + (ld)^2], \tag{2}$$

where (k, l) are the horizontal wavenumbers in the zonal (x) and meridional (y) directions, respectively, $\lambda = \sqrt{gH}/f$ is the Rossby radius of deformation, and d is the mesh spacing as per Fig. 1. The corresponding numerical dispersion relationships, using the obvious discretization for each of the five grids, are

$$\left(\frac{\omega}{f}\right)_A^2 = 1 + \left(\frac{\lambda}{d}\right)^2 [\sin^2 kd + \sin^2 ld], \tag{3a}$$

$$\left(\frac{\omega}{f}\right)_B^2 = 1 + 2\left(\frac{\lambda}{d}\right)^2 [1 - \cos kd \cos ld], \tag{3b}$$

* The U.S. Government's right to retain a nonexclusive royalty-free license in and to the copyright covering this paper, for governmental purposes, is acknowledged.

0021-9991/95 $6.00

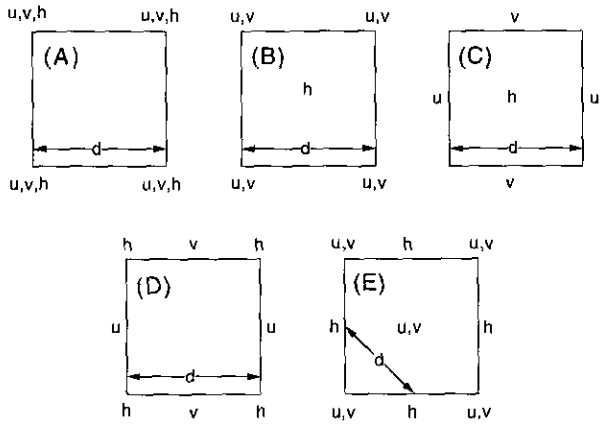

FIG. 1. Definition of Arakawa grids A–E, assuming a square grid. Here u, v are the horizontal velocity components, h is the vertical displacement, and d is the mesh spacing.

$$\left(\frac{\omega}{f}\right)_C^2 = \cos^2\frac{kd}{2}\cos^2\frac{ld}{2} + 4\left(\frac{\lambda}{d}\right)^2\left[\sin^2\frac{kd}{2} + \sin^2\frac{ld}{2}\right], \tag{3c}$$

$$\left(\frac{\omega}{f}\right)_D^2 = \cos^2\frac{kd}{2}\cos^2\frac{ld}{2} + \left(\frac{\lambda}{d}\right)^2\left[\cos^2\frac{kd}{2}\sin^2 ld + \cos^2\frac{ld}{2}\sin^2 kd\right], \tag{3d}$$

$$\left(\frac{\omega}{f}\right)_E^2 = 1 + 2\left(\frac{\lambda}{d}\right)^2\left[\sin^2\frac{kd}{\sqrt{2}} + \sin^2\frac{ld}{\sqrt{2}}\right]. \tag{3e}$$

Figures 2 and 3 plot the two-dimensional dispersion relations for the cases $\lambda/d = 2$ and $\lambda/d = 1/2$, respectively, for the exact case, as well as for the five grids. The same plots for the case $\lambda/d = 2$ are also given by Randall [5]. The origin, or the region where the discrete and exact dispersion relationships coincide, is at the lower left-hand corner. We show only the

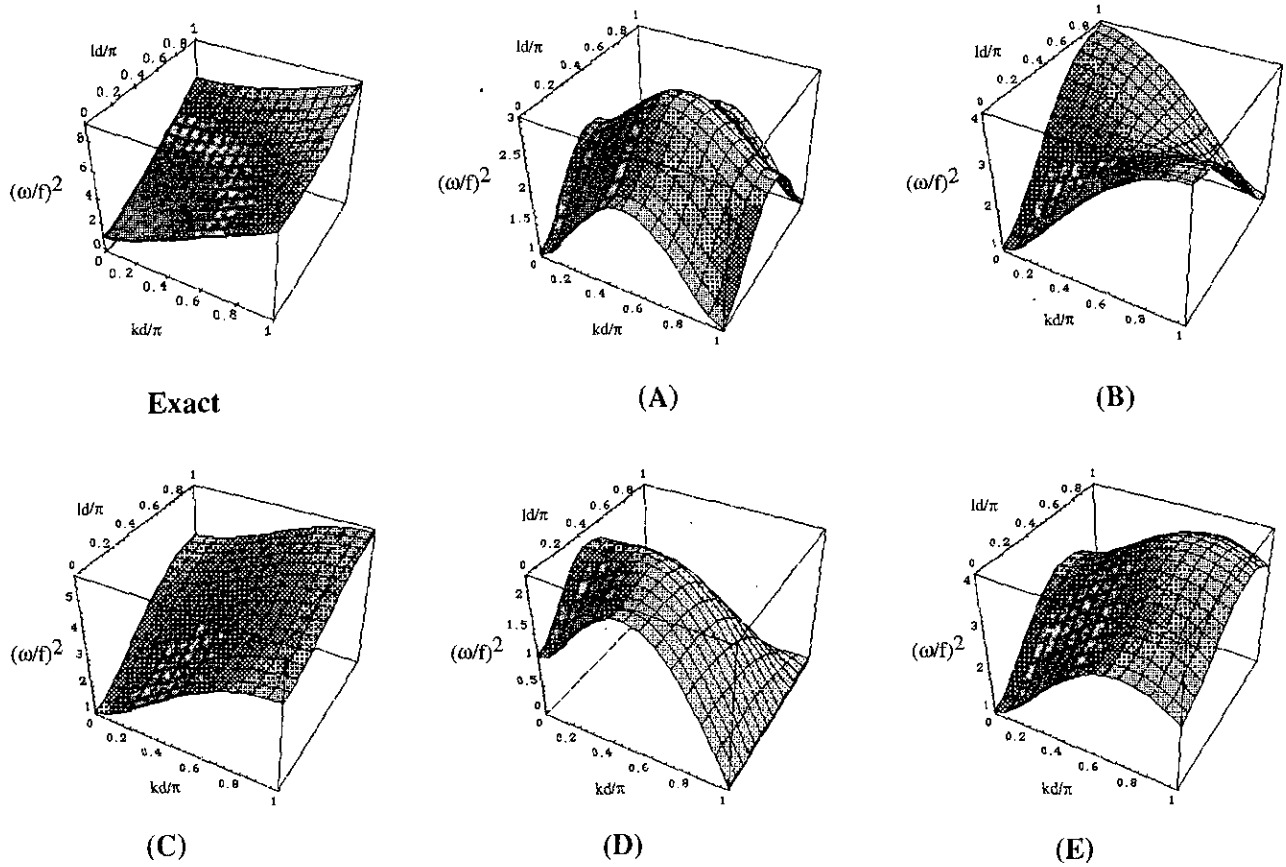

FIG. 2. Nondimensional frequency $(\omega/f)^2$ for inertia–gravity waves plotted using Eqs. (2) and (3a)–(3e) with resolved Rossby radius, $\lambda/d = 2$. The admissibility region for grids A–D is the square region $(kd/\pi, ld/\pi) < 1$ and for the E grid it is the triangular region $kd/\pi + ld/\pi < \sqrt{2}$.

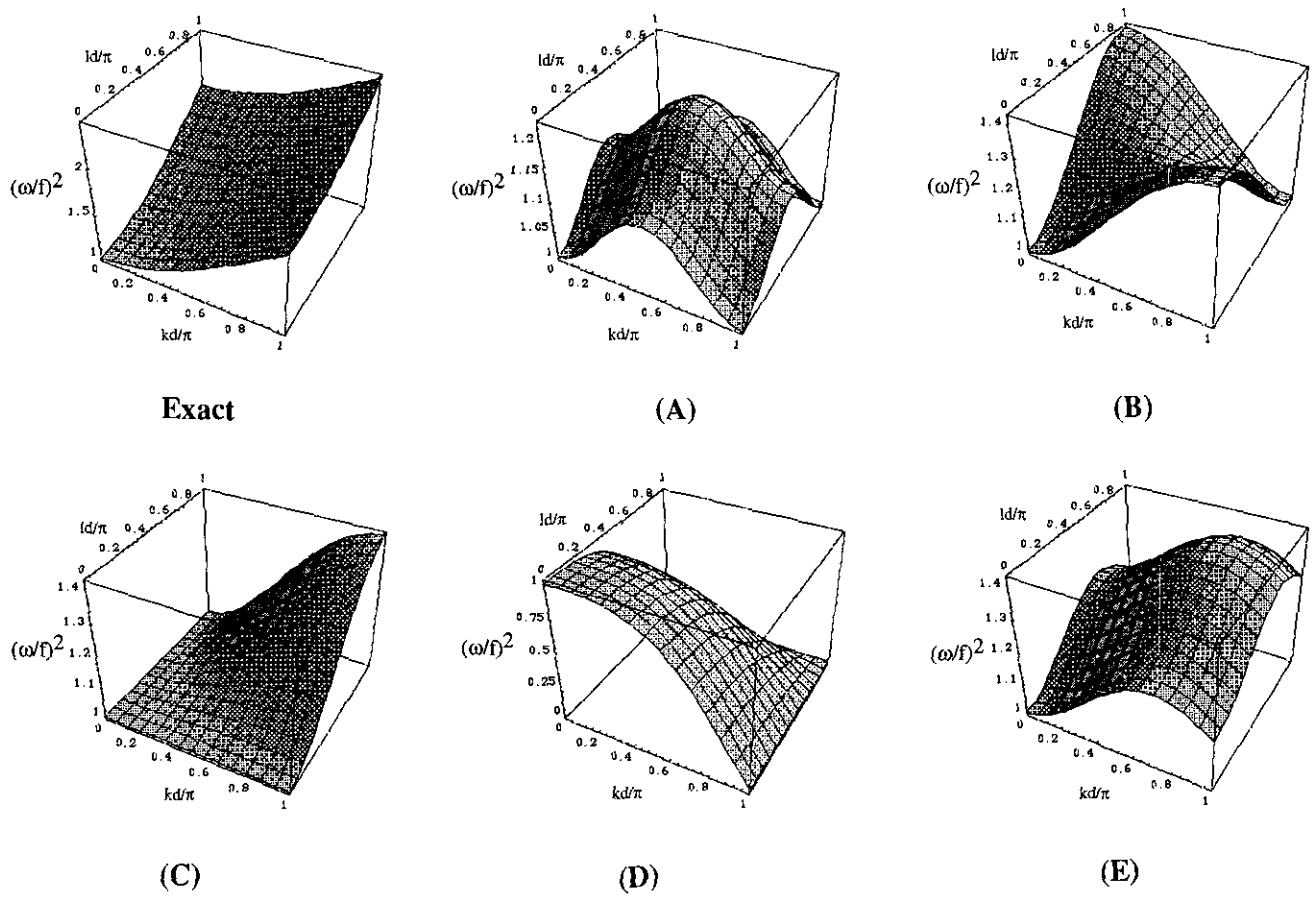

FIG. 3. Nondimensional frequency $(\omega/f)^2$ for inertia–gravity waves plotted using Eqs. (2) and (3a)–(3e) with under-resolved Rossby radius, $\lambda/d = 1/2$. The admissibility region is the same as in Fig. 2.

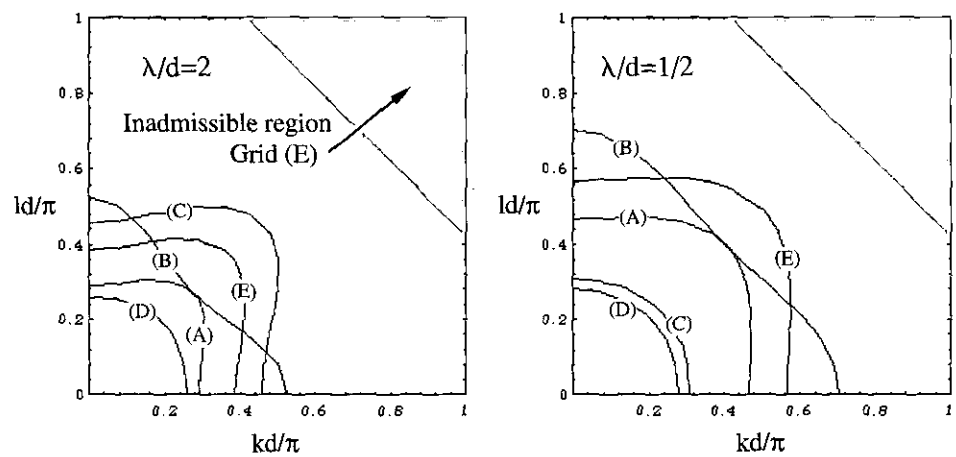

FIG. 4. Contour lines of 10% error in frequency for inertia–gravity wave dispersion relations on Arakawa A–E grids within their admissibility regions. The region from the origin up to the contour line for a particular grid constitutes the "domain of accuracy" for that grid.

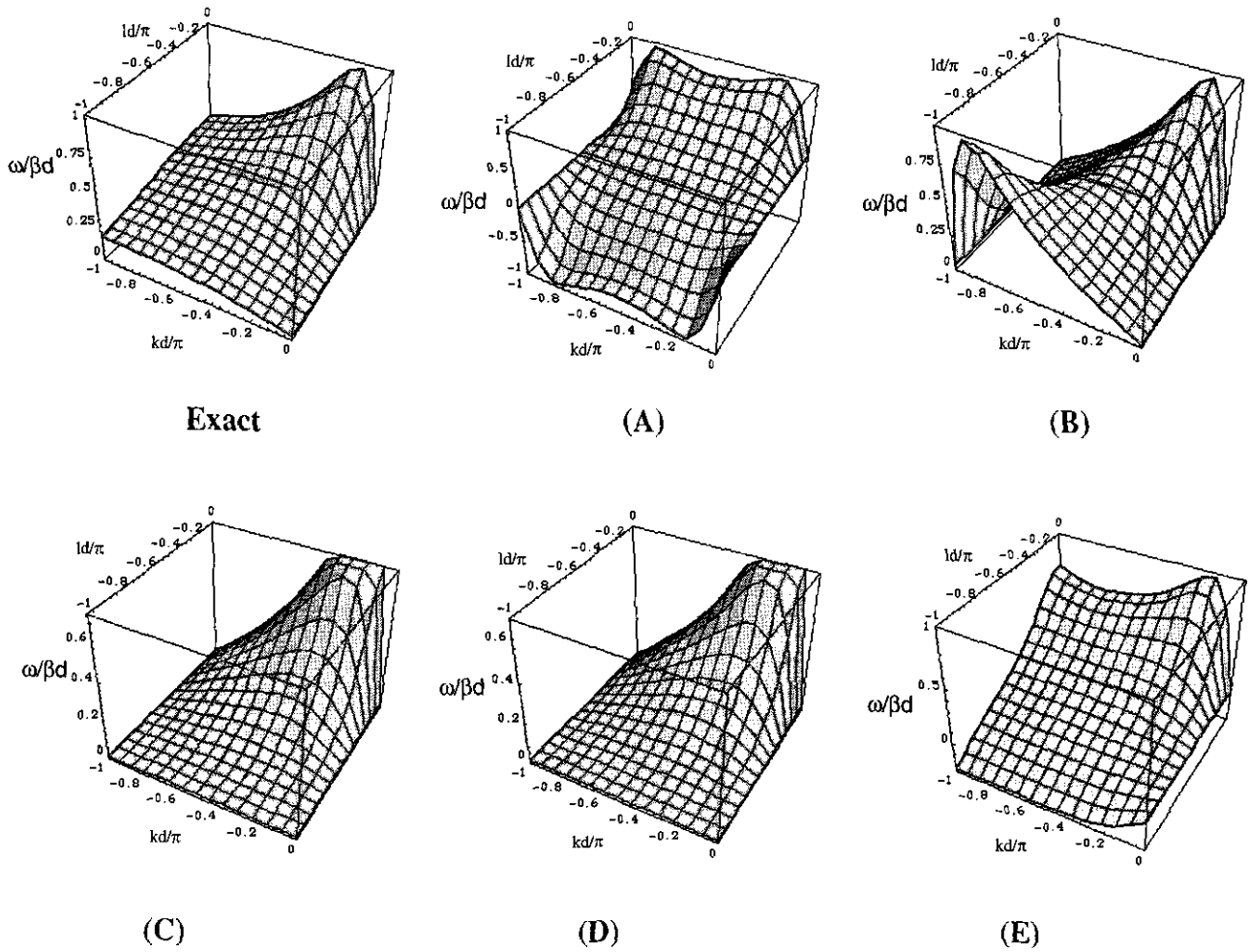

FIG. 5. Nondimensional frequency $\omega/\beta d$ for Rossby waves plotted using Eqs. (5) and (6a)–(6e) with resolved Rossby radius, $\lambda/d = 2$. The admissibility region is the same as in Fig. 2.

upper right-hand quandrant in the k, l plane; the remaining quadrants may be constructed by symmetry.

It is useful to define the region of resolvable wavenumbers for these plots, or the so-called "admissible region" [7] in wavenumber space. The admissible region for grids A–D is the square region defined by $k, l < \pi/d$, and for grid E it is the triangular region defined by $k + l < \sqrt{2}\pi/d$ (e.g., [2, 5, 7]). Combining all four quadrants of the k, l plane, the admissible region for all grids is seen to be a square with side length $2\pi/d$, but with the E grid region rotated by 45°, as is to be expected, because the E grid is the same as the B grid, except rotated by 45°. For convenience, we have displayed the same region, $k, l < \pi/d$, for all grids. Note the "null spaces" associated with the discrete spatial operators for the A and B grids at the corners of the display box in Figs. 2 and 3, with (k, l) equal to $(0, \pi/d)$, $(\pi/d, 0)$, and $(\pi/d, \pi/d)$. These represent spurious nonphysical modes, such as the "checkerboard" mode, which undergo only inertial oscillations and often account for the computational "noise" observed in calculations. The C-grid is notable for the absence of such modes.

It is not easy to compare the accuracy of the discretizations solely on the basis of Figs. 2 and 3. Arakawa and Lamb [2] in part compared the five grids on the basis of the size of the region in which the phase and group velocities are in the same direction (as in the exact case), but this is not general. In Fig. 4 we plot the 10% error contour for each of the grids, where the error is defined as $E = |(\omega - \omega_G)/\omega|$. Here ω is the exact frequency from (2) and ω_G is a grid frequency from (3a)–(3e). The region of parameter space containing both the contour line and the origin defines the "domain of accuracy" in which the accuracy is better than the chosen level, in this case 10%. This type of presentation allows one to visually judge the different grids based on the size and shape of the domain of accuracy. We confirm the original Arakawa and Lamb [2] conclusion

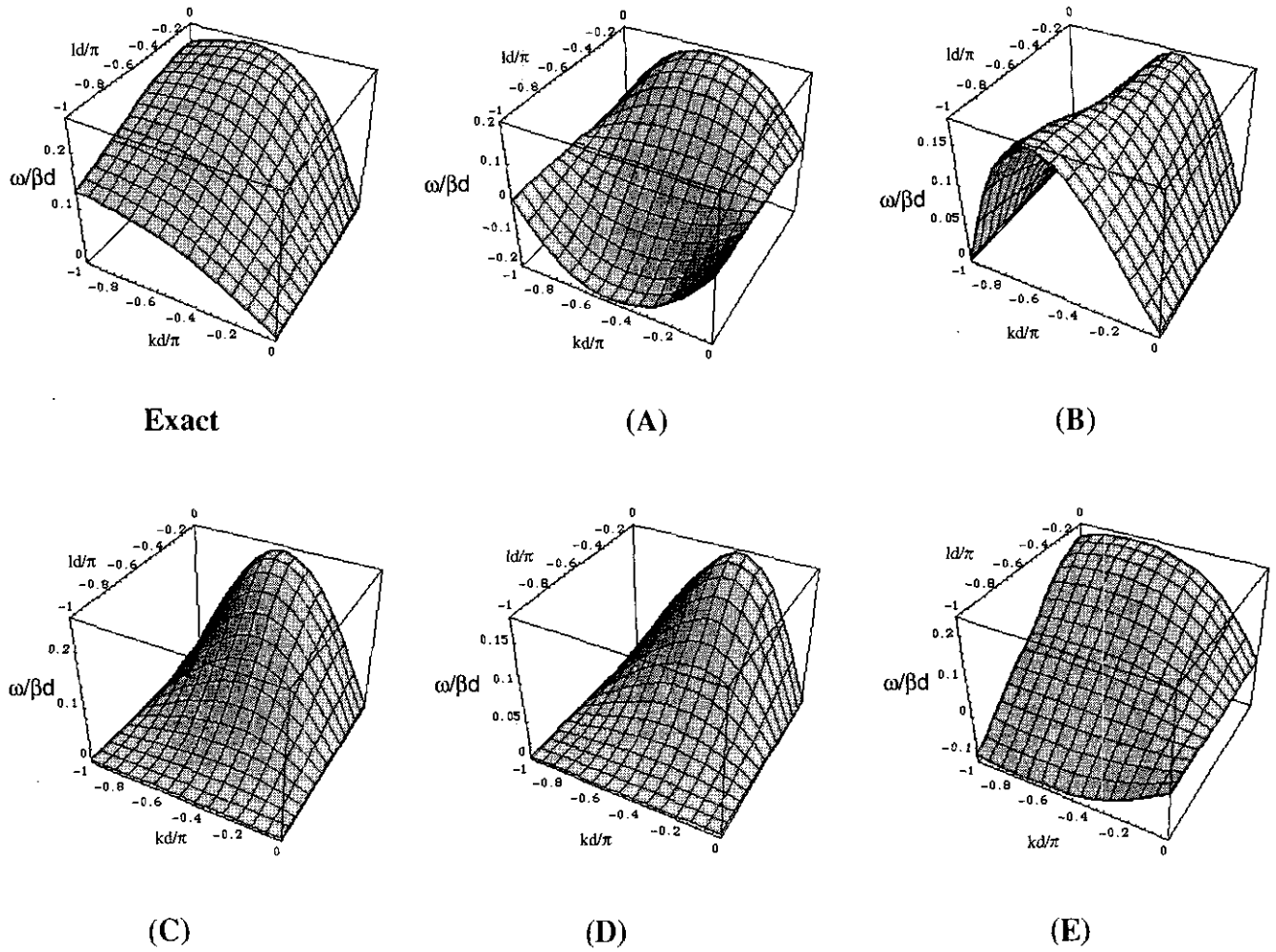

FIG. 6. Nondimensional frequency $\omega/\beta d$ for Rossby waves plotted using Eqs. (5) and (6a)–(6e) with under-resolved Rossby radius, $\lambda/d = 1/2$. The admissibility region is the same as in Fig. 2.

that the C-grid is best among the five grids for modelling geostrophic adjustment in the resolved case ($\lambda/d = 2$), while the B and E grids are better in the under-resolved case ($\lambda/d = 1/2$). Note that because inertia–gravity waves are isotropic with respect to direction, both the dispersion relations and the domains of accuracy for the B and E grids are the same, except for a rotation by 45°.

3. ROSSBY (PLANETARY) WAVES

Rossby waves in the quasi-geostrophic, β-plane approximation (Gill [8]) are given by

$$\begin{aligned} fv_g - g\partial_x h_g &= 0, \\ fu_g + g\partial_y h_g &= 0, \end{aligned} \tag{4a}$$

and

$$\begin{aligned} \partial_t u_g - fv_a - \beta v_g y &= 0, \\ \partial_t v_g + fu_a + \beta u_g y &= 0, \\ \partial_t h_g + H(\partial_x u_a + \partial_y v_a) &= 0, \end{aligned} \tag{4b}$$

where u_g, v_g, h_g are the geostrophic, u_a, v_a are the ageostrophic components of velocity and displacement, y is the meridional distance, and $\beta = \partial_y f$. Both f and β are assumed constant.

Again, assuming plane waves, we obtain the continuum (exact) dispersion relationship

$$\frac{\omega}{\beta d} = \frac{-(\lambda/d)^2\, kd}{1 + (\lambda/d)^2\,[(kd)^2 + (ld)^2]}. \tag{5}$$

The corresponding numerical dispersion relationships are

$$\left(\frac{\omega}{\beta d}\right)_A = \frac{-(\lambda/d)^2 \sin kd \cos ld}{1 + (\lambda/d)^2\,[\sin^2 kd + \sin^2 ld]}, \tag{6a}$$

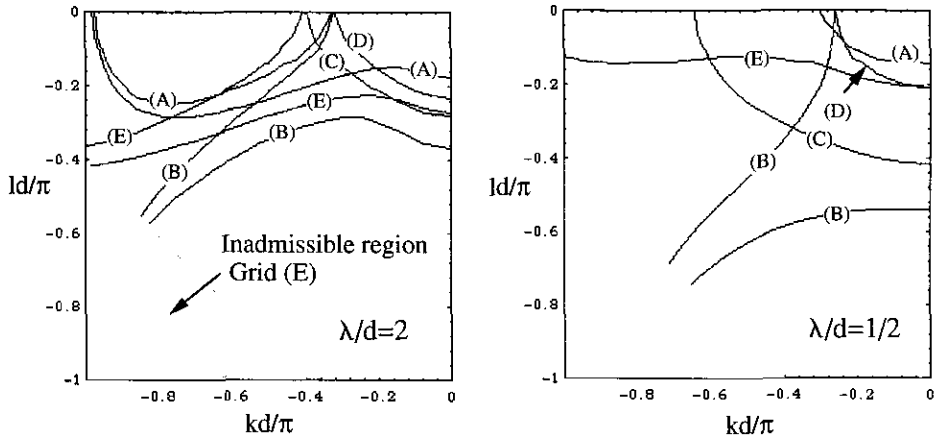

FIG. 7. Contour lines of 10% error in frequency for Rossby wave dispersion relations on Arakawa A–E grids within their admissibility regions. The region between the origin in the upper right-hand corner up to the contour line constitutes the "domain of accuracy" for a particular grid.

$$\left(\frac{\omega}{\beta d}\right)_B = \frac{-(\lambda/d)^2 \sin kd}{1 + 2(\lambda/d)^2 [1 - \cos kd \cos ld]}, \tag{6b}$$

$$\left(\frac{\omega}{\beta d}\right)_C = \frac{-(\lambda/d)^2 \sin kd \cos^2(ld/2)}{\cos^2(kd/2)\cos^2(ld/2) + 4(\lambda/d)^2 [\sin^2(kd/2) + \sin^2(ld/2)]}, \tag{6c}$$

$$\left(\frac{\omega}{\beta d}\right)_D = \frac{-(\lambda/d)^2 \sin kd \cos^2(ld/2)}{1 + 4(\lambda/d)^2 [\sin^2(kd/2) + \sin^2(ld/2)]}, \tag{6d}$$

$$\left(\frac{\omega}{\beta d}\right)_E = \frac{-\sqrt{2}(\lambda/d)^2 \sin(kd/\sqrt{2}) \cos(ld/\sqrt{2})}{1 + 2(\lambda/d)^2 [\sin^2(kd/\sqrt{2}) + \sin^2(ld/\sqrt{2})]}. \tag{6e}$$

Figures 5 and 6 plot the two-dimensional dispersion relationships for the cases $\lambda/d = 2$ and $\lambda/d = 1/2$, respectively, for all five grids and the exact case. Note that the origin is now in the upper right-hand corner. These waves propagate in a westwardly direction only (we therefore display only the lower left-hand quadrant in the k-l plane; the upper left-hand quadrant may be constructed by symmetry).

Figure 7 shows the 10% domains of accuracy for Rossby waves. In this case the B grid appears to be superior to the C grid for both resolved ($\lambda/d = 2$) and under-resolved ($\lambda/d = 1/2$) cases, except for a relatively small region containing long meridional and intermediate zonal wavelengths. The C-grid domain is more isotropic, however. Note that the D grid gives the worst accuracy, both here and in Fig. 4. Figure 8 shows the 30% domains of accuracy; note that the size of the domains is expanded but that conclusions regarding the relative effectiveness of the different grids remain unchanged. This time, because Rossby waves are not isotropic with respect to direc-

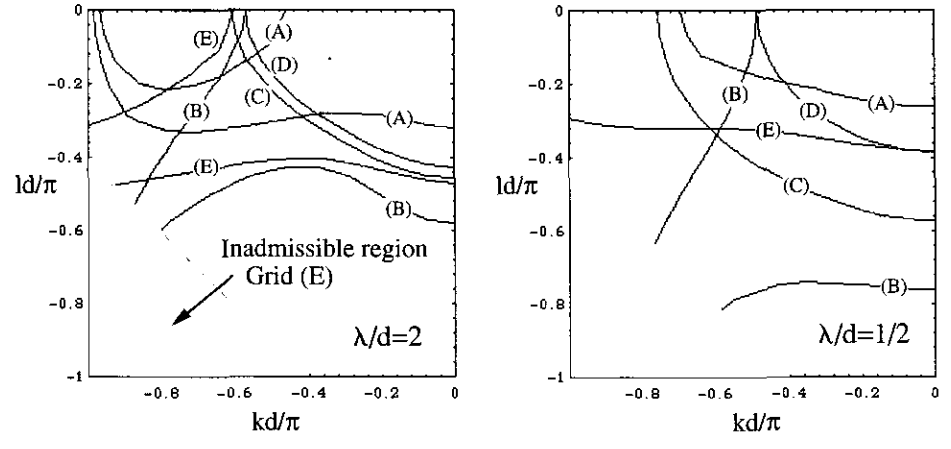

FIG. 8. Same as 7, except for 30% error contours.

tion, the dispersion relations are quite different for the B and E grids.

ACKNOWLEDGMENT

This work was supported by the CHAMMP program of the U.S. Department of Energy.

REFERENCES

1. F. J. Winninghoff, Ph.D. thesis, UCLA, 1968 (unpublished).
2. A. Arakawa and V. R. Lamb, "Computational Design of the Basic Dynamical Processes of the UCLA General Circulation Model," in *Methods of Computational Physics,* Vol. 17 (Academic Press, New York, (1977), p. 173.
3. M. L. Batteen and Y. J. Han, *Tellus* **33,** 387 (1981).
4. Y. Song and T. Tang, *J. Comput. Phys.* **105,** 72 (1993).
5. D. A. Randall, Mon. Weather Rev. **122,** 1371 (1994).
6. R. C. Wajsowicz, *J. Phys. Oceanogr.* **16,** 773 (1986).
7. F. Mesinger and A. Arakawa, *Numerical Methods used in Atmospheric Models,* Vol. 1, GARP Publ. Ser., No. 17 (WMO, Geneva, 1976), p. 45.
8. A. E. Gill, *Atmosphere–Ocean Dynamics* (Academic Press, San Diego, 1982), p. 496.